sustainability

MDPI

Article

Assessment of Formaldehyde's Impact on Indoor Environments and Human Health via the Integration of Satellite Tropospheric Total Columns and Outdoor Ground Sensors

Elena Barrese [1], Marco Valentini [1], Marialuisa Scarpelli [1], Pasquale Samele [1], Luana Malacaria [2], Francesco D'Amico [2,3,*] and Teresa Lo Feudo [2,*]

[1] Department of Medicine, Epidemiology, Occupational and Environmental Hygiene, National Institute for Insurance Against Accidents at Work, Area Industriale Comp. 15, I-88046 Lamezia Terme, Catanzaro, Italy; e.barrese@inail.it (E.B.); ma.valentini@inail.it (M.V.); m.scarpelli@inail.it (M.S.); p.samele@inail.it (P.S.)
[2] Institute of Atmospheric Sciences and Climate, National Research Council of Italy, Area Industriale Comp. 15, I-88046 Lamezia Terme, Catanzaro, Italy; l.malacaria@isac.cnr.it
[3] Department of Biology, Ecology and Earth Sciences, University of Calabria, Via Bucci Cubo 15B, I-87036 Rende, Cosenza, Italy
* Correspondence: f.damico@isac.cnr.it or francesco.damico@unical.it (F.D.); t.lofeudo@isac.cnr.it (T.L.F.)

Abstract: Formaldehyde (HCHO) is harmful to human health and an adequate assessment of its concentrations, both in outdoor and indoor environments, is necessary in the context of sustainable policies designed to mitigate health risks. In this research, ground indoor and outdoor HCHO measurements are integrated with the analysis of tropospheric total columns obtained by satellite surveys to assess the concentrations of HCHO in a number of environments, exploiting the proximity of a World Meteorological Organization—Global Atmosphere Watch (WMO/GAW) observation site in Calabria, Southern Italy to a National Institute for Insurance against Accidents at Work (INAIL) department in the municipality of Lamezia Terme. The meteorological parameters used by the WMO station are also used to provide additional data and test new correlations. Using statistical significance tests, this study demonstrates the presence of a correlation between indoor and outdoor HCHO concentrations, thus showing that an exchange between indoor and outdoor formaldehyde does occur. Rooms located in the local INAIL building where indoor measurements took place also demonstrate degrees of susceptibility to HCHO exposure, which are correlated with the orientation of prevailing wind corridors in the area. The new findings constitute an unprecedented characterization of HCHO hazards in Calabria and provide regulators with new tools with which to mitigate formaldehyde-related risks.

Keywords: Lamezia Terme; formaldehyde; sustainability; SP5; indoor air quality; outdoor air quality; urban planning

Citation: Barrese, E.; Valentini, M.; Scarpelli, M.; Samele, P.; Malacaria, L.; D'Amico, F.; Lo Feudo, T. Assessment of Formaldehyde's Impact on Indoor Environments and Human Health via the Integration of Satellite Tropospheric Total Columns and Outdoor Ground Sensors. *Sustainability* **2024**, *16*, 9669. https://doi.org/10.3390/su16229669

Academic Editors: O. V. Giannico, Roberta Zupo and Maria Lisa Clodoveo

Received: 23 October 2024
Revised: 1 November 2024
Accepted: 4 November 2024
Published: 6 November 2024

1. Introduction

Formaldehyde (HCHO or CH_2O) (FA), one of the most common volatile organic compounds (VOCs), is a colorless, irritating, and extremely volatile gas [1]. Assessments of the health hazards posed by the presence of formaldehyde in indoor environments have been performed for decades, with early research works on the issue proposing threshold values related to exposure [2] and the means of risk mitigation [3]. Consequent research further demonstrated the consequences of HCHO exposure to human health in indoor environments [4–6]. In a study by Schmitz et al. (2000), the hypothesis that plants could purify indoor air up to a level that could limit harmful FA exposure was effectively disproven [7], thus showing that actual risk mitigation practices and policies were necessary. Over the years, methods of detecting indoor formaldehyde concentrations improved in accuracy, sampling rate, and applicability, thus providing new tools for use towards a better understanding of FA exposure hazards in a number of indoor environments [8,9] and their

variability across countries [10–12]. In 2004, formaldehyde was included in Group 1 by the International Agency for Research on Cancer (IARC) [13], who defined it based on scientific evidence as a carcinogen for humans. Subsequent investigations (monograph 100F of 2012) confirmed this classification. This confirmation was based on sufficient epidemiological evidence to determine that FA causes leukemia and the death of the nasopharynx [14,15]. The European Commission classified formaldehyde as a carcinogen (Category 1B), as a mutagen (Category 2), and as acutely toxic (Category 3) in June 2014 [16].

Over the years, exposure to this molecule has been linked to indoor air pollution, with the WHO raising concerns about its negative health effects [17]. Millions of people in modern society spend about 90% of their time indoors [18–20]. In Italy, research has also focused on monitoring indoor air quality, especially in buildings of critical importance, such as hospitals and schools [21].

Numerous health risks are associated with poor indoor air quality (IAQ), a parameter that is representative of indoor air and its effects of human comfort and health. It can be affected by various factors such as wood-based building materials, paper products, personal care products, tobacco smoke, and inadequate HVAC (heating, ventilation, and air conditioning) systems [22–30].

There are also several outdoor sources of FA. Anthropogenic sources include vehicle emissions, biofuel and coal combustion, industrial processing, and wood-based building materials; this compound is also released due to secondary formation from other reactive volatile organic compounds [31–36]. Wildfires also contribute to significant FA emissions in the atmosphere, and the consequent diffusion of air masses and plumes can significantly expand the areas affected by direct FA exposure [37–45]. In addition to anthropogenic pollution, the location (e.g., whether an area is rural or urban), temperature, relative humidity, wind regime, cloud cover, season, and time of day can all influence the concentration of formaldehyde in ambient air [46–51]. FA has also been confirmed to be present in outer space, being found in areas ranging from interplanetary to interstellar environments [52–55].

With respect to absolute concentrations, those of indoor FA are higher than their outdoor counterparts [56–66]: in the conventional indoor environment, average concentrations are typically about 20–40 $\mu g/m^3$, while outdoor concentrations hover around 1–4 $\mu g/m^3$; lower concentrations are reported in rural areas, while higher levels are observed in polluted cities [67].

The WHO [68] have established an indoor air quality guideline for formaldehyde, but there is no similar guideline for outdoor air, even though it is considered a toxic air contaminant. This lack of outdoor guidelines makes it difficult to assess the potential indoor contributions of outdoor formaldehyde. Recent studies have examined the relationship between indoor and outdoor air to investigate how outdoor formaldehyde affects indoor concentrations; the results from leading studies show that outdoor formaldehyde can make a significant contribution to indoor levels [69].

Due to the limited availability and spatial variability of ground-based measurements, some studies have used satellite data to map outdoor surface formaldehyde concentrations [69–71].

This research study aims to investigate the long-term outdoor contribution of formaldehyde to indoor concentrations by correlating satellite data with outdoor and indoor measurements. Total column data are frequently used in research to gather data that would not otherwise be obtainable by surface measurements alone [72]. In this research, HCHO column data from Sentinel-5P VCD have been used to map surface air HCHO concentrations and connect them to ground data in the Mediterranean region, where this field of research is new. Because the formaldehyde concentration in indoor air is usually inversely correlated with the air exchange rate, measurements of microclimatic parameters and air exchange were carried out.

This study, based on a 2021 measurement campaign performed in Lamezia Terme (Calabria, Southern Italy), is divided as follows: Section 2 describes the sites where the

campaign took place and their peculiarities, and also highlights the instruments and methods used for measurement; Sections 3 and 4 show the results of the evaluation and their discussion, respectively; Section 5 concludes the paper.

2. Experimental Campaign Sites, Instruments, and Methods

2.1. Experimental Campaign Sites

An experimental campaign was performed in 2021 at the coastal infrastructure of INAIL's DiMEILA (National Institute for Insurance against Accidents at Work—Department of Medicine, Epidemiology, Occupational and Environmental Hygiene) and the WMO/GAW (World Meteorological Organization—Global Atmosphere Watch) regional station of Lamezia Terme (code: LMT), operated by the National Research Council of Italy—Institute of Atmospheric Sciences and Climate (CNR-ISAC), located nearby. The GAW experimental site (Lat: 38.88 °N; Lon: 16.24 °E) is located 600 m from the Tyrrhenian coastline of Calabria at an elevation of 6 m above sea level. The Catanzaro isthmus between the Tyrrhenian and Ionian seas is the narrowest point in the entire Italian peninsula, with a distance of approximately 31 km between the two coastlines (Figure 1); the isthmus separates the Serre Massif, located in the South, from the coastal chain (*Catena Costiera*) in the northwest and the Sila Massif in the North. The particular orographic configuration of the isthmus results in well-defined W/NE wind circulation, which is characterized by moderate wind breezes from the sea (NW–SW), mainly developed during daytime, while northeastern gentle wind breezes from the land mainly affect the nighttime period [73,74]. Over the course of LMT's observation history, local wind circulation was further characterized using LiDAR and other techniques [75–77]. The 10/28 (100/280 °N) runway orientation of the Lamezia Terme International Airport (IATA: SUF; ICAO: LICA), located 3 km north from the INAIL and ISAC research centers, also shows that local air traffic is subject to the same wind regimes affecting atmospheric measurements at the GAW site.

The LMT station, located within Lamezia Terme's industrial area, is influenced by various sources of anthropogenic emissions: the research on greenhouse and reactive gasses performed at ISAC since 2015 indicates that the airport, the A2 highway, livestock farming, and agriculture are emission sources in the area [78]. Research on case studies also showed relevant inputs from Saharan dust events [79] and summer open-fire emissions [80]. A study on seven years of methane data showed that northeastern continental winds were enriched with CH_4, while western seaside winds yielded lower values; in addition to that, low-speed winds from the northeast were linked to the highest observed mole fractions. The opposite held true also: high-speed winds from the same air corridor were linked to low concentrations [81]. A consequent study on surface ozone (O_3), however, showed a reversed pattern, thus demonstrating that each atmospheric compound can have peculiar impacts on local observations [82].

Research on LMT data also relied on new methods to differentiate between natural and anthropogenic emissions by highlighting weekly cycles. In fact, while natural emissions are affected by daily to yearly cycles, anthropogenic emissions show weekly variations, attributable to different anthropic activities throughout the week. Following cross-station studies on aerosols and their anthropogenic emission sources [83,84], another study evaluated weekly patterns in unprecedented detail at LMT and also proposed a new methodology for similar assessments on a global scale [85]. Additional and new insights on local emission sources were possible thanks to an environmental evaluation of the first 2020 COVID-19 lockdown period in Italy: with anthropic activities reduced to a minimum under those exceptional circumstances, several emission sources in the area could be pinpointed [86]. New research has focused on the peplospheric or PBL (Planetary Boundary Layer) influence on the surface concentrations of key pollutants under different wind regimes [87].

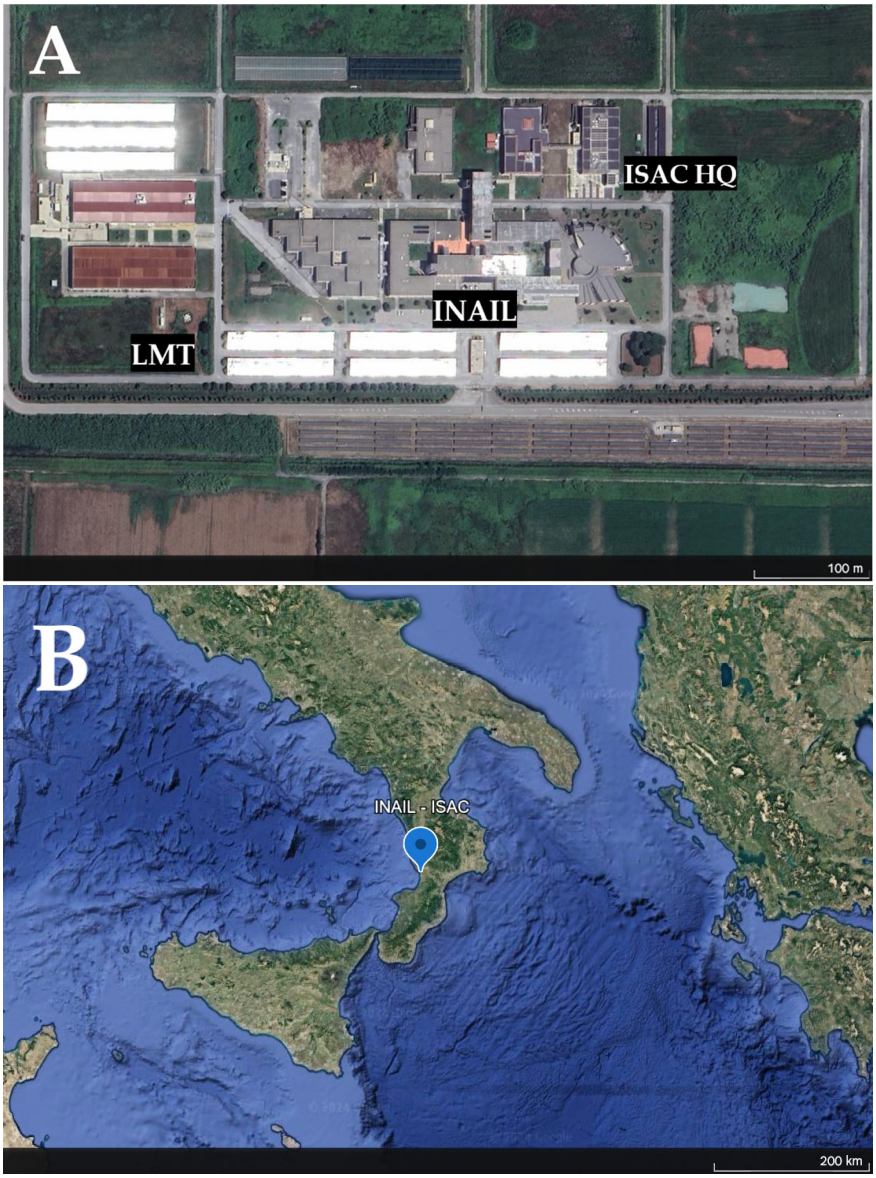

Figure 1. (**A**) Details on the location of both research centers in the industrial area of Lamezia Terme. (**B**) Location of the two research centers in southern Italy.

2.2. Total Tropospheric Vertical Column (TVC) Density of HCHO as Assessed by Satellite

Satellite outdoor measurements of the total vertical column density (TVC) of formaldehyde (HCHO) in the troposphere have been carried out using the Sentinel-5P satellite, a global air pollution monitoring satellite launched by ESA on 13 October 2017 as part of the Copernicus mission [88]. Sentinel-5P uses a high inclination orbit (about 98.7°), defined as the angular distance of an orbital plane from the equator. Sentinel-5P's has a sun-synchronous, near-polar orbit. This orbit leads 5P to cross the equator at 13:30 MLST (Mean Local Solar Time); this implies that the surface of the Earth is always illuminated, at the same angles, by the Sun. The total orbit of 5P is 16 days (14 orbits per day, or 227 orbits per cycle) and the orbital reference altitude is approximately 824 km. The advanced Tropospheric Monitoring Instrument (TROPOMI), used for the detailed atmospheric measurements carried out onboard Sentinel-5P, is located in a low Earth orbit in the afternoon polar region with a swath width of 2600 km. There are four spectrometers, each electronically split into two bands (two channels in SWIR, two channels in VIS, two channels in UV, and two channels in NIR), with radiometric accuracies in absolute terms of 1.6% (SWIR) and 1.9% (UV) compared to Earth's spectral reflectance. With the finest spatial resolution of

3.5 × 5.5 km^2 and a high signal-to-noise ratio compared to the most advanced atmospheric monitoring spectrometers currently available, the instrument has been performing global scans since August 6th, 2019. Operational Level 2 (L2) products are currently available to the public and several research works in the literature cover the results obtained via their use [89–91].

2.3. Indoor and Outdoor Sampling Sites, Instruments and Times

Regarding indoor monitoring, a total of twelve office rooms, one room used with photocopiers, and one was a large training room (often used to host external events) were investigated from March to June 2021. The samplings were carried out during normal working activities, reproducing a real indoor workplace environment representative of standard employee risk to FA exposure. A typical time point (09:00–13:00 A.M.) was identified to characterize the diurnal working trend. The samplers were placed on the desk close to the worker, one meter away from the walls of each room. In smaller offices, one sampling point was used; however, in larger rooms two points were subject to these measurements. Three samples were taken at each sampling point over three consecutive days. The furniture provided for each workstation comprised a desk, a bookcase, and a chest of drawers. All offices have windows and a centralized air recycling system.

In conjunction with indoor formaldehyde measurements, samplers were placed outside the structure on a terrace adjacent to the monitored offices at a height of 1.5 m. In addition to HCHO monitoring, comprehensive microclimatic measurements were taken at both indoor and outdoor locations with a sampling rate of once per minute. Furthermore, the indoor air exchange rate from the recycling system was assessed.

Indoor microclimatic measurements were performed using two integrated data loggers (LSI-LASTEM model M-Log—ELO009–Settala, Italy), each equipped with a psychrometric sensor mod. The mod used was an ESU102A, which acquired wet and dry forced ventilation temperatures according to the ISO7726 standard [92]. They were also equipped with a hot wire anemometer mod; this was an ESV308, which was used for measuring mean air speed and turbulence intensity at a high rate. The measurement precision of the employed psychrometers is ±0.1 °C for temperature and ±2% for RH (relative humidity) in the temperature range of 5–45 °C, while the anemometer has an accuracy of ±0.06 m/s in the 0.1–4 m/s range and one of ±0.08 m/s in the range of 0.4–3.0 m/s.

The instruments were positioned on a tripod at a height of approximately 1.5 m, and were kept close to the sampling system indoor measurement points. The acquisition rate was 1 second for each parameter, and after 60 s of continuous measurement, the averages were stored in the aboard memory. In addition to measuring microclimatic conditions, a balometer TSI Accubalance 8380 (Shoreview, Minnesota, USA) was used to measure the air flux from a ceiling-mounted cassette air conditioner when operating.

Outdoor meteorological measurements were performed by the station located in the same area in which the chemical measurements were acquired. Since 2015, several instruments have been in operation at the WMO/GAW LMT as part of a number of different monitoring programs. In this study, we used an automatic weather station (Vaisala WXT520–Vantaa, Finland) to collect data at a height of 10 m above ground level. This station, which is part of the WMO/GAW instrument pool, records meteorological parameters such as wind velocity (m/s), direction (°), temperature (°C), relative humidity (%), barometric pressure (hPa), and accumulated rainfall (10 min averages). The wind sensor consists of an array of three ultrasonic transducers that are equally spaced out in a horizontal plane: the time required for ultrasound waves to travel from one transducer to the other two was used by the instrument to determine wind speed and direction. The precipitation sensor was used to detect the impact of individual rain drops and the generated signals were proportional to drop volume; this allowed the signal from each drop to be converted directly into the amount of accumulated rainfall. An advanced RC oscillator and two reference capacitors were used to continuously measure the capacitance of the pressure, temperature, and humidity sensors. The temperature dependence of the pressure

and humidity sensors is compensated by the transmitter's microprocessor, thus allowing the instrument to detect ambient air pressure, RH, and temperature with a sampling rate of one minute between measurements.

2.4. Outdoor Tropospheric TVC Formaldehyde Satellite Methods for Data Processing

In accordance with technical documents and recommendations, offline TROPOMI L2 HCHO data gathered between 1 March and 31 August 2021 were used in this research. HCHO data were provided in either in mol/m^2 or in molecule/cm^2 using a multiplication factor of 6.02214×10^{19}, as suggested by ESA [93]. An algorithm programmed in MATLAB-R2016a, comprising several consecutive digital processing steps, was used to reprocess the data stream and HCHO column data.

The algorithm operates as follows: daily TROPOMI data are downloaded in a netCDF format; these data are parsed through and all required variables are processed; coordinates (latitude, longitude) and time are extracted and converted according to the satellite's tracking and scanning time; gas data are extracted from the global matrix and consequently stored in an array focused on a particular region of interest; the array is therefore georeferenced and all values with a Q_a value less than 0.5 are excluded. This step is in accordance with the recommendations on TROPOMI data processing, as the quality of data is normally indicated by assigning a value ranging from 0 to 1 for all registered columns, and only columns with a Q_a greater than 0.5 are recommended (meaning a cloud radiance fraction at 340 nm < 0.5, no error flag, surface albedo $\leq$ 0.2, no snow/ice warning, Solar Zenith Angle (SZA) $\leq 70^{\circ}$, and air mass factor > 0.1) [94,95].

The algorithm includes a function aimed at performing a direct comparison between a target site located at precise coordinates and satellite measurements in its vicinity. The method ultimately relates the minimum distance to the target site to the smallest distance datum in the array used for processing.

2.5. Formaldehyde Indoor/Outdoor Surface Analysis Methods

Indoor and outdoor formaldehyde were sampled using personal sampling pumps equipped with adsorbent tubes, containing a front bed of 300 mg DNPH-coated silica gel and a back bed of 150 mg DNPH-coated silica gel [96]. The tubes were eluted with 5 mL of HPLC-grade acetonitrile (ACN) and analyzed using an HPLC Shimadzu (model LC-20 AB – Kyoto, Japan) coupled with a binary pump and UV-VIS detection (SPD-20 A/AV) at a wavelength of 365 nm. A calibration curve with an R^2 value of 0.9994 was established to quantify formaldehyde concentrations. The detection limit for formaldehyde was 0.02 µg/mL, and the recovery rate was 90–105%.

DNPH (2,4-Dinitrophenylhydrazine) cartridges are devices used for air sampling purposes. They were specifically designed for sampling carbonyls such as HCHO. Carbonyls compounds are trapped by high-purity silica adsorbent coated with 2,4-dinitrophenylhydrazine. In this trap, they are converted into hydrazone derivatives, which in turn are eluted from the cartridge in acetonitrile and are analyzed by HPLC. Once the sample has been injected into HPLC, chromatographic separation takes place, whereby the carbonyl compounds captured by the vial transform into hydrazones. Consequently, a chromatogram in which they are perfectly separated is generated. This allows the dual qualitative and quantitative analysis of each parameter via a calibration curve previously plotted using certified standards.

2.6. Statistical Methods

Statistical analysis was performed on the chemical and physical parameters and some correlation tests were performed. These evaluations were performed in Jamovi v. 2.3. With regard to the meteorological and microclimatic parameters (outdoor and indoor), the first step was to organize homogeneous datasets starting from raw data and then aggregate them on an hourly basis for all the parameters considered: outdoor temperature—T_{out} °C; indoor temperature—T_{ind} °C; outdoor relative humidity—RH_{out}%;

indoor relative humidity—RH_{in}%; outdoor wind speed and direction—WS_{out} and WD_{out}; indoor wind speed—WS_{in}; and indoor wind direction—WD_{in}. Following the aggregation of all considered meteorological parameters on an hourly basis, a homogeneous dataset is organized, starting with the raw data gathered every one minute. Statistical methods for quality control and validation are applied to the raw data to remove outliers and problems that may be due to technical issues.

In order to perform comparisons between concentrations of formaldehyde accumulated between 11:00 and 15:00 UTC, the mean and standard deviation (SD) were calculated, starting from the hourly mean homogenized dataset of the interval between 11:00 and 15:00 UTC. The Spearman's rank correlation coefficient (SR) [97,98] was then applied to these new datasets. The SR is a method used to test the strength and direction (positive or negative) of the correlation, whether related or associated, between two variables, and this technique is called Pearson's correlation coefficient between ranked variables [99]. For a sample of size *n*, the variables x and y are converted into the ranks R_x and R_y, respectively, and the SR coefficient, ρ, is calculated as follows:

$$\rho = (\mathrm{cov}(R_x,R_y))/(\sigma R_x\ \sigma R_y) \quad (1)$$

where cov is the covariance of the rank variables and σR_x and σR_y are the standard deviations of the rank variables. The Spearman's rank correlation can have a value ranging from +1 to −1 and its interpretation is similar to that of the PCC (Pearson correlation coefficient).

3. Results

3.1. Outdoor Formaldehyde

The possibility of studying atmospheric concentrations at LMT, in the absence of the previous and continuous measurement of formaldehyde, is enabled by the use of satellite data. On the basis of this information, we performed an analysis of the outdoor HCHO tropospheric column provided by the SP5 mission, using the methodology described in Section 2.5, between 1 March and 31 August 2021.

Seasonal variations in environmental parameters and FA concentrations are shown in Figure 2. The daily mean TVC density values HCHO were used to compute monthly and seasonal averages, along with median values and percentile thresholds (5th, 25th, 75th, and 95th percentiles). A seasonal trend emerged, with higher monthly mean formaldehyde concentrations observed during warm summer months. The highest monthly average TVC density HCHO value, $1.3 \times 10^{16} \pm 0.6 \times 10^{16}$ molecules/cm^2 (blue spots), was recorded in July 2021, whereas lower concentrations were detected in March and April.

In Figure 3, surface and columnar data measured at the satellite's passage by the experimental site are highlighted, and a single datum per day can be compared directly with the in situ data. The comparison between surface measurements and the satellite dataset showed that regarding the recorded outdoor HCHO concentration peaks, an increase is observed in both cases, with a similar trend.

This data evaluation emphasizes the importance of combining satellite observations with ground-level measurements to obtain a comprehensive understanding of formaldehyde distribution and its influencing factors, particularly in complex environments like the Mediterranean region; research previously carried out at LMT on multi-year datasets of continuous measurements. The results evidenced opposite surface concentration patterns for methane [81] and ozone [82], thus showing that these concentrations need to undergo enhanced analyses to be adequately assessed.

In Figure 4, we reported the indoor and outdoor average concentrations of formaldehyde detected in each room within the INAIL research center in Lamezia Terme. In general, indoor concentrations of FA are higher compared to their outdoor counterparts.

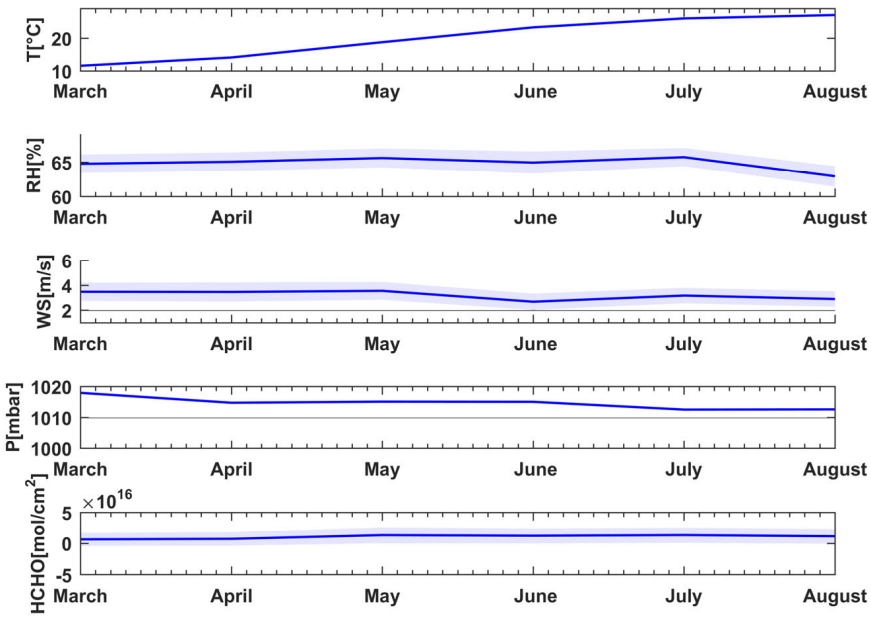

Figure 2. Monthly environmental and HCHO values observed at the site during the 2021 campaign. From top to bottom, we show the temperature (°C), relative humidity (%), wind speed (m/s), pressure (mbar), and TVC density HCHO count (molecules/cm^2). Shaded areas, where present, show error bars.

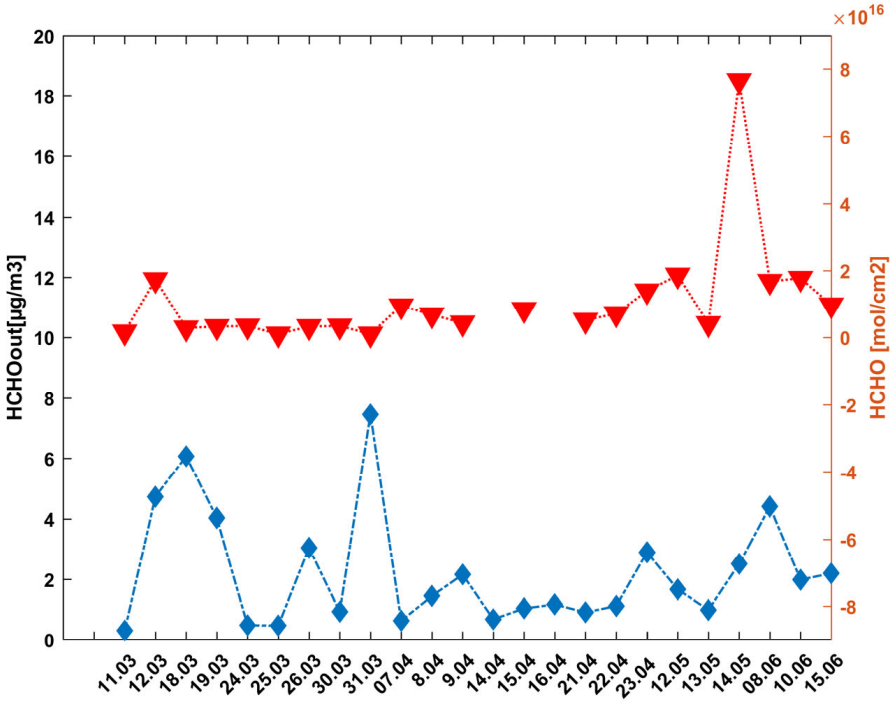

Figure 3. Comparison between near-surface outdoor HCHO cumulated concentrations values in µg/m^3 (blue line) at LMT and tropospheric column density in molecules/cm^2 (red points), as assessed by TROPOMI L2 at 13:00 local time.

In order to investigate possible correlations between meteorological/microclimatic variables, and formaldehyde concentrations during the sampling campaign, we calculated Spearman and significance tests in Jamovi following the descriptions reported in Section 2.6. The results are shown in Table 1.

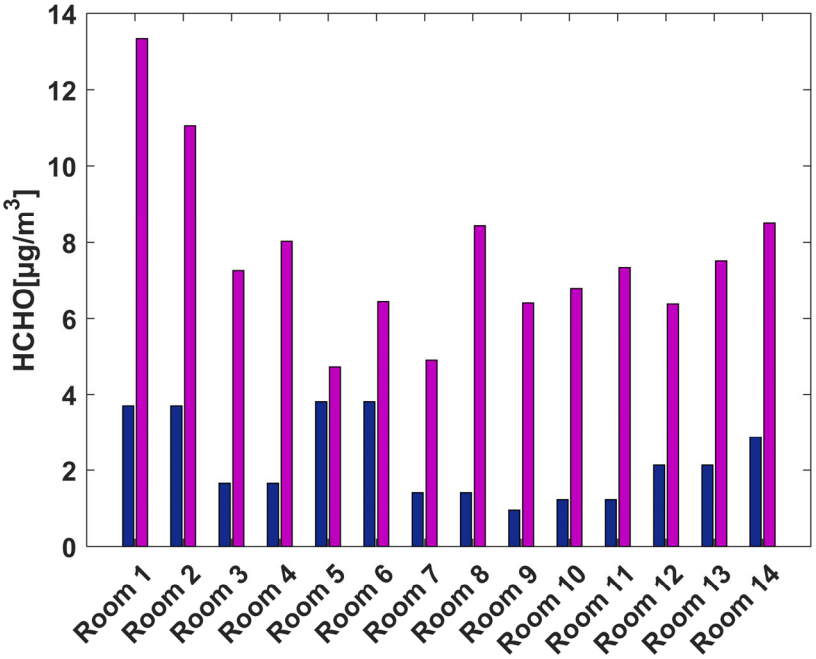

Figure 4. Comparison of outdoor and indoor HCHO concentrations in all rooms subject to the 2021 campaign. Purple bars indicate indoor concentrations, while blue bars indicate outdoor values.

Table 1. Spearman regression matrix between outdoor microclimatic parameters and HCHO external concentrations.

	$HCHO_{out}$	TVC FA	$T_{out.}$	$RH_{out.}$	WS_{out}
HCHOout	–				
TVC FA	0.169	–			
T_{out}	0.168	0.550 ***	–		
$RH_{out.}$	0.392 **	0.164	0.293 *	–	
WS_{out}	−0.130	0.106	−0.301 *	0.202	–

* $p < 0.05$, ** $p < 0.01$, *** $p < 0.001$.

The data reported in Table 1 show ρ Spearman values, while footnotes (*) indicate the statistical significance level of each test. The formaldehyde outdoor concentration is well correlated with relative humidity, with a *p*-value of 0.006, whereas the total column density of HCHO is highly correlated with external temperature, yielding a *p*-value of < 0.001.

The Spearman's test values reported in Table 2 indicate that outdoor FA concentrations are well correlated (*p*-value = 0.008) with their indoor counterparts. This holds for the indoor RH with outdoor temperature and relative humidity *p*-value, respectively (< 0.001). Furthermore, the analysis shows a weak but likely negative correlation between indoor FA concentration and indoor speed.

Table 2. Spearman's regression matrix between all the indoor and outdoor measurements.

	T_{in}	RH_{in}	WS_{in}	$T_{out.}$	RH_{out}	WS_{out}	$HCHO_{in}$	$HCHO_{out}$
T_{in}	–							
RH_{in}	0.019	–						
WS_{in}	0.029	−0.082	–					
T_{out}	0.405 **	0.654 ***	0.030	–				
RH_{out}	−0.051	0.642 ***	−0.141	0.293 *	–			
WS_{out}	−0.103	0.082	−0.098	−0.301 *	0.202	–		
$HCHO_{in}$	−0.057	0.276	−0.298 *	0.000	0.254	0.244	–	
$HCHO_{out}$	−0.086	0.293	−0.130	0.168	0.392 **	−0.130	0.377 **	–

* $p < 0.05$, ** $p < 0.01$, *** $p < 0.001$.

3.2. Integration of Meteorological Parameters

Accounting for the addition of Vaisala WXT520 meteorological data, a cross-evaluation was performed for 24 days between 11 March and 15 June 2021. From the analysis of surface meteorological data shown in Figure 5, we note four different types of wind regime, which were also observed in recent peplospheric assessments at the same site [87]: well-developed sea–land breeze cycles with the wind direction shifting between west and east during daytime (sea breeze with onshore flow) and nighttime (land breeze with offshore flow), respectively; (green box) not complete (NC) sea–land breeze, i.e., where wind direction during night comes from south; (black box) synoptic wind flow from the west (synoptic wind); wind direction coming from the East (during night). From the data shown in Figure 5, we observed a daily cycle in the time series of physical parameters. During the night and early morning, the surface layer is stable while, during the central hours of the day, the surface layer is neutral or unstable, depending on theweather conditions.

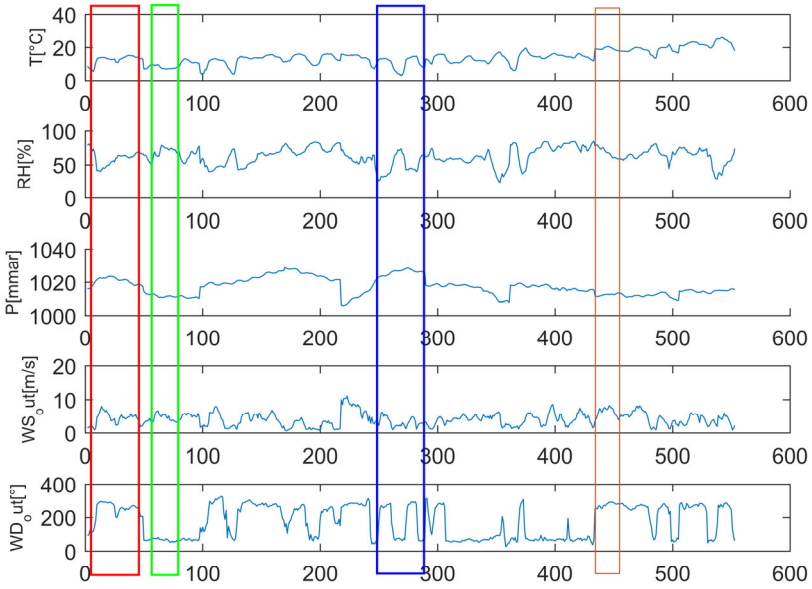

Figure 5. Daily wind regimes throughout the campaign, which are distributed as follows: breeze (blue box); not complete (NC) breeze (red box); western synoptic flow (orange box); eastern synoptic flow (green box). Additional evaluations on the effects of these regimes on local observations are available in D'Amico et al. (2024e) [87].

Looking at the acquired data and examining each day of the campaign, a bivariate statistical analysis shows how local winds affect the in situ outdoor FA. A bivariate statistical analysis is used to provide useful evidence to assist in investigations of how local winds affect outdoor FA when observed by in situ measurements. To this end, daily surface HCHO values are analyzed as a function of wind speed and direction, observed at an LMT station during the experimental campaign (Figure 6). The highest HCHO concentrations (>5 $\mu g/m^3$) occur with winds blowing from east–northeast (E-NE) (Figure 6), a pattern that is in accordance with the methane peaks at the same site described in D'Amico et al. (2024a) [81].

The findings shown in Figure 6 suggest that inland air masses play a key role in promoting the occurrence of elevated levels of these atmospheric tracers under local circulation conditions (mountain breeze, wind speed < 5 m/s). A cyclonic event characterized by higher wind speeds is associated with the lower values observed for this air mass's provenance. In general, two different situations occur when considering the west and southwest (W-SW) sectors: the first is linked to the establishment of the breeze regime, with winds below 6 m/s, characterized by the transport of sea spray, which occurs most frequently at LMT, especially in spring and summer; the second is related to the synoptic conditions with wind speeds above 8 m/s, which are characterized by the transport of

different types of gasses and aerosols into the atmospheric column. With this wind regime, several events transporting aerosols from the Sahara [79] and volcanic ash from Etna and Stromboli—located nearby at a distance of 2 km, 3357 m above sea level, and at a distance of 1 km, 924 m above sea level, from the site offshore [80], respectively—are observed. In addition, CO and CO_2 are transported. This is especially true in summer due to the frequent fires that occur in the Calabrian region [80]. In Figure 7, scatter plots have been computed to test the correlation between indoor and outdoor HCHO concentrations, and a number of meteorological parameters.

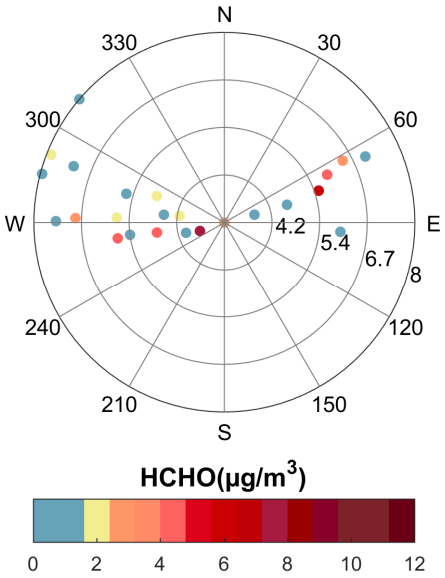

Figure 6. Results of bivariate analyses on accumulated daily values of HCHO surface outdoor concentration as a function of wind speed and direction during the day of the monitoring campaign.

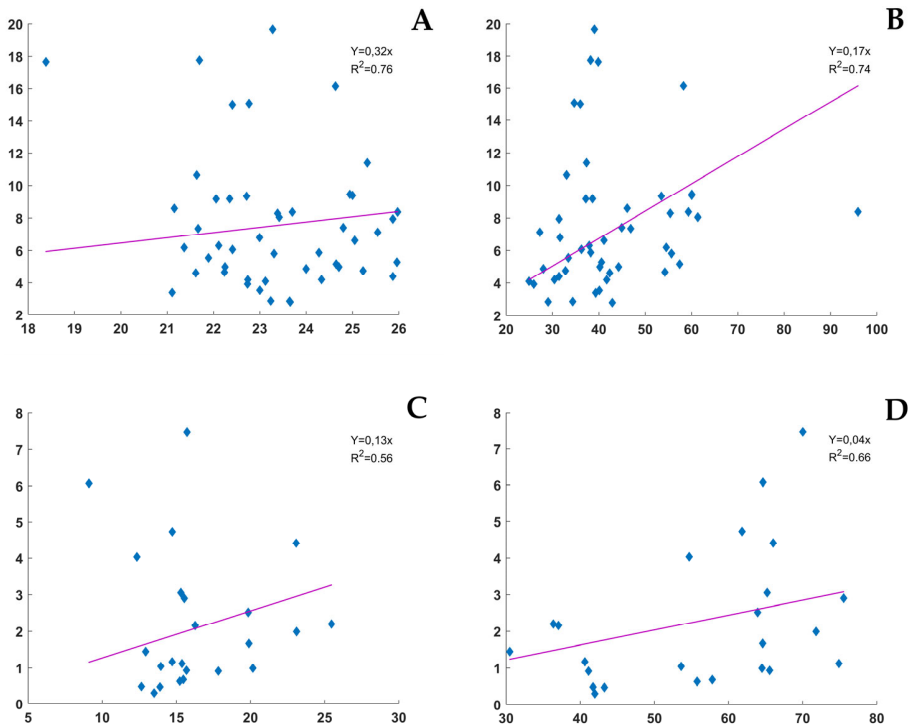

Figure 7. Correlation scatter plots between HCHO (indoor and outdoor) concentrations and meteorological parameters. (**A**) T_{ind} vs. $HCHO_{ind}$; (**B**) RH_{ind} vs. $HCHO_{ind}$; (**C**) T_{out} vs. $HCHO_{out}$; (**D**) RH_{out} vs. $HCHO_{out}$.

In detail, during the study, the relevant influence of wind circulation on the monitored site was observed. In Figure 8, the average concentrations of indoor and outdoor HCHO in each working room and outdoor wind speed, determined based on wind direction, are reported.

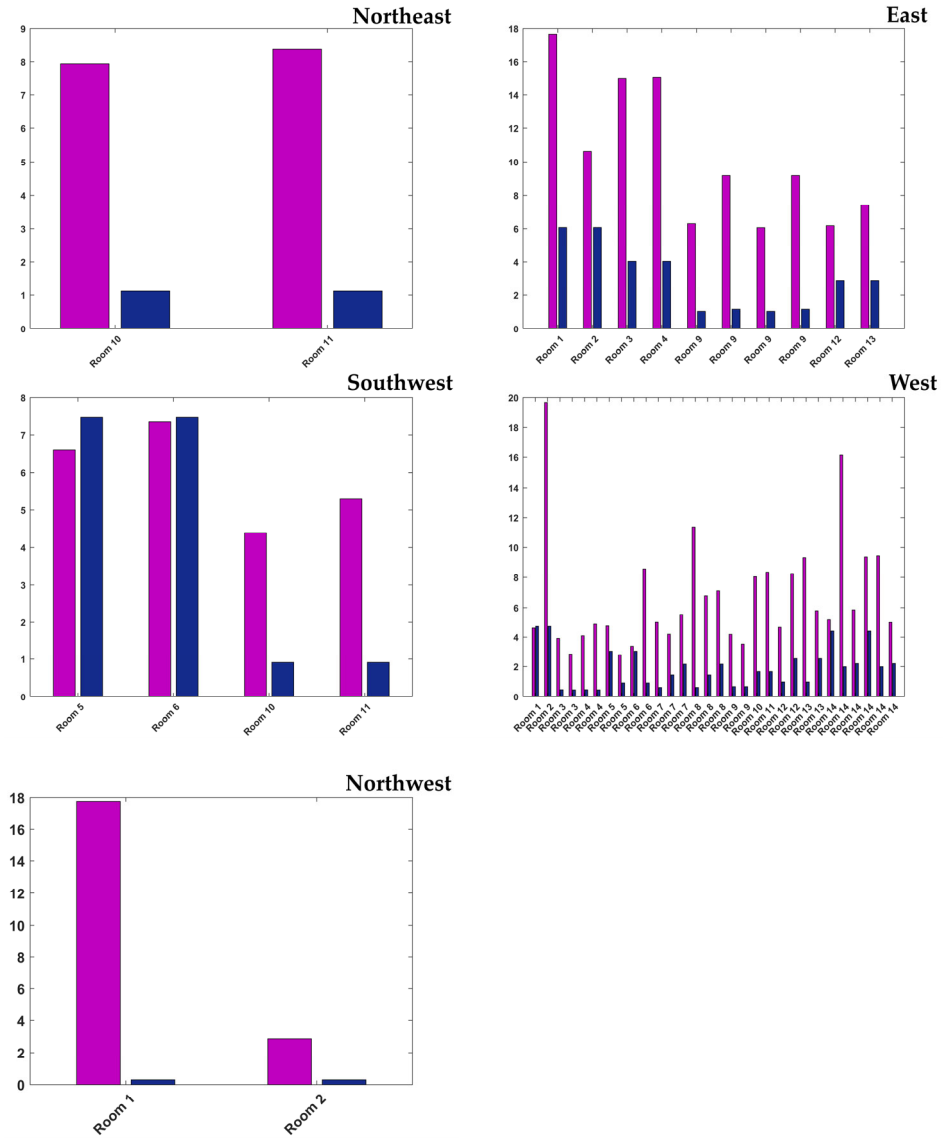

Figure 8. Correlations between surface outdoor/indoor formaldehyde and wind parameters by wind sector. Purple bars indicate indoor concentrations, while blue bars indicate outdoor values.

As already stated, indoor HCHO concentrations are always higher than outdoor mole fractions; however, in case of E-NE wind corridors, such differences are amplified due to anthropic pollution. Details on the observed O/I (outdoor to indoor) ratios are given in Figure 9.

The outdoor/indoor concentration ratio is commonly reported to be less than 1, indicating that indoor formaldehyde concentrations are typically higher than those found outdoors. The surveyed rooms generally had O/I values below the 1 threshold; rooms 1, 5, 6, and 7 were close to this threshold, thus indicating similar outdoor and indoor FA concentrations.

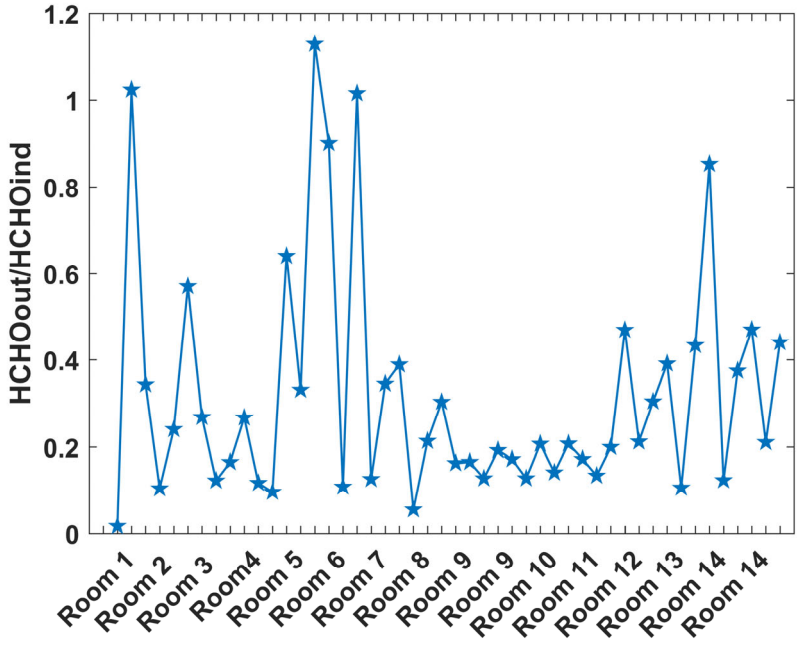

Figure 9. Outdoor to indoor (O/I) ratios of formaldehyde, per room.

4. Discussion

In the industrial area of Lamezia Terme (Calabria, Southern Italy), a joint campaign by INAIL's DiMEILA (Department of Medicine, Epidemiology, Occupational and Environmental Hygiene—National Institute for Insurance against Accidents at Work) and CNR's ISAC (National Research Council of Italy—Institute of Atmospheric Sciences and Climate) research centers (Figure 1) assessed formaldehyde concentrations during summer 2021 by integrating satellite data with local measurements. This experimental campaign, performed during the 2021 summer season, is a first step towards the joint indoor/outdoor assessment of FA exposure hazards in Calabria, which would provide policy makers and regulators with new tools aimed at the development of new and efficient sustainable policies. A proper evaluation of FA exposure is required, as atmospheric measurements in the region report notable wildfire emissions [80], which are among the sources of FA report in the literature (Section 1).

The need to perform integrated satellite/ground evaluations of FA ahead of more detailed analyses has been highlighted in the literature [100–103]. These two-pronged analyses provide data in circumstances where surface measurements are limited to ground observations [44,69].

In this work, satellite data from Sentinel-5P on atmospheric column were integrated by local surface measurements of formaldehyde (HCHO, FA) and key meteorological parameters (temperature, wind speed and direction, relative humidity) (Figure 2) to assess the indoor and outdoor exposure to FA in areas not subject to continuous measurements (Figure 3). Indoor analyses were performed on a per-room basis at the INAIL research center (Figure 4) in order to add a new degree of detail to the study.

The site where the campaign took place is located on the Tyrrhenian coast of Calabria, in the municipality of Lamezia Terme, and previous works on the site have shown the presence of well-established wind regimes dominated by breezes and prevailing W/NE corridors [73,74]. These have a strong influence on the atmospheric concentration of greenhouse gasses and pollutants observed at the local WMO/GAW station [81,82,87]. Prevailing wind regimes were classified and used to determine the main corridors of air mass transport in order to test their influence on formaldehyde concentrations in the campaign (Figure 5).

In the W/NW sector, outdoor FA concentrations are lower due to seaside winds, which are generally depleted in terms of pollutants [81], although exceptions such as surface

ozone (O_3) have been reported [82]. The W/SW sectors yield higher outdoor and indoor concentrations, which we hereby attribute to orthopedic prosthetics manufacturing in that direction. Specifically, the W sub-sector yields lower values compared to the SW sub-sector because wind speeds in the latter direction are lower and air masses can persist for a longer period of time, thus increasing the exposure and detection times. This finding in particular corroborates previous research performed at the CNR-ISAC WMO/GAW regional station [82] and proves the susceptibility of buildings to local wind circulation patterns. In the context of urban planning, enhanced susceptibility to these patterns and increased indoor pollution need to be considered by policy makers and regulators.

Near-surface outdoor HCHO cumulated concentrations show a peak, as shown in Figure 3. It was verified that on March 31st, a date coinciding with that peak, the orthopedic prosthetics manufacturing process was intense, an occurrence that combined with a low-speed southwestern wind to increase the local persistence of HCHO peaks linked to prosthetics manufacturing.

Regarding the reliability of total tropospheric column data obtained via TROPOMI L2 measurements, they are subject to corrections, processing algorithms, and adjustments that are relevant to the purpose of this work. In fact, L2 data on HCHO do not have the same degree of sensitivity throughout the vertical column, as the instrument is more sensitive to surface and near-surface formaldehyde concentrations compared to their high-altitude counterparts. Although high-altitude FA data are still considered reliable, L2's sensitivity to surface and near-surface concentrations further corroborates the effectiveness of the correlations with outdoor ground measurements.

Overall, the correlation between concentrations and wind parameters (Figure 6) is in accordance with other studies, performed at the WMO site, on how local wind circulation affects surface observations of greenhouse gasses and pollutants. Specifically, methane showed a HBP (Hyperbola Branch Pattern) sensu D'Amico et al. (2024a, 2024c) [81,86], with low concentrations linked to higher wind speeds, indicating remote sources, and the highest concentrations linked to low wind speeds, correlated with local sources. In particular, the pattern was prominent in northeastern continental winds enriched in anthropogenic pollutants. Formaldehyde, in this integrated study, follows a similar pattern which is distinct from that observed for ozone at the same site [82]. These findings display the susceptibility of buildings to FA exposure with respect to prevailing local wind regimes, and also add degrees of variability which are correlated with meteorological factors observed on a local scale, such as relative humidity and temperature (Figure 7). With respect to microclimatic parameters and their influence on indoor FA concentrations (Figure 7A,B), a positive correlation was observed between indoor formaldehyde and both temperature and relative humidity. This finding highlights the importance of FA exposure risk mitigation on a per-room basis. Indoor FA is often released from building materials, furniture, and other sources in office environments. As the temperature rises, these materials release more formaldehyde, leading to higher indoor concentrations. Humidity interacts with formaldehyde-releasing materials (like particleboard, or wood products) and increases FA emission rates. Water molecules in the air facilitate formaldehyde's release, and also increase its indoor concentrations. Humid air itself can also retain more formaldehyde, thus intensifying the effect of indoor pollution in humid conditions. For offices and comparable rooms, this is especially relevant in climates with seasonal humidity spikes or in poorly ventilated buildings where humid conditions can persist for long periods of time. The effects of outdoor temperature and relative humidity on outdoor HCHO were also examined, as shown in Figure 7C,D. A slightly positive correlation is observed, which is hereby deemed attributable to photochemical reactions, which in turn are correlated with temperature and sunlight intensity.

The correlations tested in Figure 7 show the presence of outliers, which are hereby attributed to additional contributions to HCHO concentrations in addition to those tested by the plots, thus indicating the presence of multiple external factors which can influence formaldehyde concentrations in similar environments.

Outdoor and indoor FA showed an average correlation rate, thus indicating an exchange between the two environments. With respect to external relative humidity, FA showed a correlation. Indoor and outdoor RH values were also correlated, thus indicating the lack of AC in the surveyed rooms.

Research indicates that outdoor formaldehyde concentrations generally vary, ranging between 3 and 20 $\mu g/m^3$. These are influenced by factors such as industrial activities, vehicular emissions, and meteorological conditions. Conversely, indoor levels frequently range from 20 to 100 $\mu g/m^3$, with notable peaks in environments where formaldehyde-emitting products are prevalent. The O/I ratio, defined as the ratio between outdoor and indoor FA concentrations observed in this study, shows the contribution of outdoor FA to observed indoor concentrations. An O/I ratio of 0.3, for example, indicates that 30% of indoor FA has an outdoor origin, while the remaining 70% is present due to indoor sources such as furniture. Furthermore, the O/I ratio can fluctuate based on ventilation practices, seasonal changes, and building (in this case, room) occupancy levels.

It is known from the key literature that the significant increase in indoor formaldehyde concentrations relative to outdoor levels is attributed to several factors (Section 1). Poor ventilation increases the indoor accumulation rate of FA because it reduces air exchange. In outdoor environments, air flows lead to dilution and dispersion. Indoor environments are characterized by a number of sources, ranging from building materials to household products used on a daily basis; smoking and cooking, which are typical human activities, also result in FA indoor release.

Seasonal influences can also lead to changes in FA concentrations, as higher outdoor temperatures may trigger photochemical reactions capable of perturbing FA levels.

This study was limited to the summer, which still allowed us to highlight patterns and the interplay of several factors: the O/I ratios shown in Figure 9 allow us to determine the presence of rooms which are more likely to be exposed to FA hazard and rooms with such exposure (specifically, their orientation and position within the building) are correlated with certain wind directions and local wind circulation. The findings of this campaign would still be applicable to local sustainable policies meant to mitigate FA risks.

The decision to perform a boreal summer campaign was based on HCHO seasonal changes, which show the influences of higher temperatures on formaldehyde emissions and releases [104,105].

A proper understanding of O/I levels on a per-room scale are deemed significant for a proper assessment of the FA exposure hazard. As a confirmed carcinogen, FA should be monitored constantly, and concentration peaks require precise and immediate action to mitigate all related risks. The findings of this study show that gathering data in one spot within a building is not sufficient to determine the broad FA hazard, as individual rooms need to be considered, as well as their orientation with respect to prevailing winds. The findings shown in this study therefore constitute a new foundation upon which FA exposure hazards assessments should be based on.

5. Conclusions

A joint venture campaign performed by INAIL DiMEILA and CNR ISAC in the municipality of Lamezia Terme (Calabria, Southern Italy) exploited the presence of a WMO/GAW observatory located near a research center specialized in insurance against accidents at work. Local meteorological data gathered at the WMO observation sites were used in conjunction with the results of a campaign on indoor and outdoor formaldehyde (FA) concentrations to assess, for the first time, correlations between key meteorological parameters and FA exposure in outdoor and indoor environments. In addition to surface data, total column data from the Sentinel-5P satellite were used to further assess correlations between the findings and third-party data. Due to the vertical sensitivity variability of satellite data, surface and near-surface measurements of formaldehyde in the vertical column are more influential in TROPOMI L2 data, hence the higher degrees of correlation with surface data gathered by ground sensors. The application of algorithms to these

measurements further strengthened their correlation with surface data on HCHO gathered by ground sensors.

The campaign shows the correlation between indoor and outdoor FA, defined as an O/I ratio indicating the exchange between the two surveyed environments. This study was aimed at specific rooms within the INAL building and demonstrated the heterogeneity of FA exposure hazards. O/I values were demonstrated to vary, even in the context of the same building, above and below the O/I threshold of 1.

Furthermore, rooms were proven to have different degrees of susceptibility to FA exposure depending on their orientation to prevailing wind circulation pattern. This was in accordance with previous research at the WMO site, which showed well-defined correlations between wind patterns and the concentrations of greenhouse gasses and other pollutants.

This study shows the importance of integrating, where available, data from other sources to complement indoor and outdoor FA assessments and provides new insights on sustainable regulations and policies that could be channeled towards the mitigation of the FA exposure risk in workplaces and similar environments. This study therefore establishes the foundation for gaining new insights on sustainable urban planning in the southern Italian region of Calabria and other regions characterized by similar outdoor formaldehyde exposure hazards and climates.

Author Contributions: Conceptualization, E.B., M.V. and T.L.F.; methodology, E.B., M.V., M.S., P.S. and T.L.F.; software, T.L.F.; validation, E.B., M.V., M.S., P.S., L.M. and T.L.F.; formal analysis, E.B., M.V., M.S., P.S., L.M. and T.L.F.; investigation, E.B., M.V., M.S., P.S., L.M. and T.L.F.; data curation, E.B., M.V., P.S., L.M. and T.L.F.; writing—original draft preparation, E.B., M.V., M.S., P.S., F.D. and T.L.F.; writing—review and editing, E.B., M.V., M.S., P.S., L.M., F.D. and T.L.F.; visualization, F.D. and T.L.F.; supervision, E.B., M.V. and T.L.F.; funding acquisition, E.B., M.V. and T.L.F. All authors have read and agreed to the published version of the manuscript.

Funding: This research was funded by INAIL (Italian National Institute for Insurance against Accidents at Work) and CNR-ISAC (National Research Council of Italy—Institute of Atmospheric Sciences and Climate).

Institutional Review Board Statement: Not applicable.

Informed Consent Statement: Not applicable.

Data Availability Statement: The datasets mentioned in this work are not readily available because they are currently being evaluated for ongoing research. Sentinel-5P data are accessible via the platforms linked in this paper.

Acknowledgments: The authors would like to acknowledge the support of Claudia Roberta Calidonna (PI of the Lamezia Terme WMO/GAW observation site) and Ivano Ammoscato (technical supervisor at the same WMO site). The authors would also like to acknowledge the three anonymous reviewers who contributed to improve and expand the manuscript.

Conflicts of Interest: The authors declare no conflicts of interest.

References

1. Frankforter, G.B. On the Liberation of Formaldehyde Gas. *J. Am. Chem. Soc.* **1906**, *28*, 1512. [CrossRef]
2. Andersen, I.; Lundqvist, G.R.; Molhave, L. Formaldehyde in the home atmosphere. Proposed introduction of limits for airborne contaminants. *Ugeskr. Laeger* **1979**, *141*, 966–971.
3. Niemelä, R.; Vainio, H. Formaldehyde exposure in work and the general environment. Occurrence and possibilities for prevention. *Scand. J. Work Environ. Health* **1981**, *7*, 95–100. [CrossRef] [PubMed]
4. Merchán, M.L.; De La Serna, J. Formadehyde as an indoor pollutant. *Toxicol. Environ. Chem.* **1986**, *13*, 17–25. [CrossRef]
5. Schachter, E.N.; Witek, T.J.; Tosun, T.; Leaderer, B.P.; Beck, G.J. A study of respiratory effects from exposure to 2 ppm formaldehyde in healthy subjects. *Arch. Environ. Health* **1986**, *41*, 229–239. [CrossRef] [PubMed]
6. Paustenbach, D.; Alarie, Y.; Kulle, T.; Schachter, N.; Smith, R.; Swenberg, J.; Witschi, H.; Horowitz, S.B. A recommended occupational exposure limit for formaldehyde based on irritation. *J. Toxicol. Environ. Health* **1997**, *50*, 217–264. [CrossRef]
7. Schmitz, H.; Hilgers, U.; Weidner, M. Assimilation and metabolism of formaldehyde by leaves appear unlikely to be of value for indoor air purification. *New Phytol.* **2000**, *147*, 307–315. [CrossRef]

8. Gillett, K.W.; Kreibich, H.; Ayers, G.P. Measurement of indoor formaldehyde concentrations with a passive sampler. *Environ. Sci. Technol.* **2000**, *34*, 2051–2056. [CrossRef]
9. Chuah, Y.K.; Fu, Y.M.; Hung, C.C.; Tseng, P.C. Concentration variations of pollutants in a work week period of an office. *Build. Environ.* **1997**, *32*, 525–540. [CrossRef]
10. Koeck, M.; Pichler-Semmelrock, F.P.; Schlacher, R. Formaldehyde—Study of indoor air pollution in Austria. *Cent. Eur. J. Public Health* **1997**, *5*, 127–130.
11. Hong, E.; Lee, E.; Kim, Y.; Oh, E.; Kim, Y.W.; Moon, K.W.; Choi, J.W.; Lee, J.; Roh, J. The correlations between oxidative stress markers and indoor volatile organic compounds among the general population in Ansan and Incheon cities, Korea. *Toxicol. Environ. Health Sci.* **2009**, *1*, 37–48. [CrossRef]
12. Hun, D.E.; Siegel, J.A.; Morandi, M.T.; Stock, T.H.; Corsi, R.L. Cancer risk disparities between Hispanic and non-hispanic white populations: The role of exposure to indoor air pollution. *Environ. Health Perspect.* **2009**, *117*, 1925–1931. [CrossRef] [PubMed]
13. International Agency for Research on Cancer. *IARC Classifies Formaldehyde as Carcinogenic to Humans*; World Health Organization: Geneva, Switzerland, 2004.
14. Binazzi, A.; Mensi, C.; Miligi, L.; Di Marzio, D.; Zajacova, J.; Galli, P.; Camagni, A.; Calisti, R.; Balestri, A.; Murano, S.; et al. Exposures to IARC Carcinogenic Agents in Work Settings Not Traditionally Associated with Sinonasal Cancer Risk: The Experience of the Italian National Sinonasal Cancer Registry. *Int. J. Environ. Res. Public Health* **2021**, *18*, 12593. [CrossRef] [PubMed]
15. Checkoway, H.; Dell, L.D.; Boffetta, P.; Gallagher, A.E.; Crawford, L.; Lees, P.J.S.; Mundt, K.A. Formaldehyde exposure and mortality risks from acute myeloid leukemia and other lymphohematopoietic malignancies in the US National Cancer Institute Cohort study of workers in formaldehyde industries. *JOEM* **2015**, *57*, 785–794. [CrossRef] [PubMed]
16. European Union. Commission Regulation (EU) No 605/2014 of 5 June 2014 Amending, for the Purposes of Introducing Hazard and Precautionary Statements in the Croatian Language and Its Adaptation to Technical and Scientific Progress, Regulation (EC) No 1272/2008 of the European Parliament and of the Council on Classification, Labelling and Packaging of Substances and Mixtures Text with EEA Relevance. Available online: http://data.europa.eu/eli/reg/2014/605/oj (accessed on 10 October 2024).
17. World Health Organization. *WHO Guidelines for Indoor Air Quality: Selected Pollutants*; World Health Organization: Geneva, Switzerland, 2010; p. 454.
18. Brasche, S.; Bischof, W. Daily time spent indoors in German homes—Baseline data for the assessment of indoor exposure of German occupants. *Int. J. Hydrogen Environ. Health* **2005**, *208*, 247–253. [CrossRef] [PubMed]
19. Schweizer, C.; Edwards, R.; Bayer-Oglesby, L.; Gauderman, W.J.; Ilacqua, V.; Jantunen, M.J.; Lai, H.K.; Nieuwenhuijsen, M.; Künzli, N. Indoor time–microenvironment–activity patterns in seven regions of Europe. *J. Expo. Sci. Environ. Epidemiol.* **2007**, *17*, 170–181. [CrossRef]
20. Mannan, M.; Al-Ghamdi, S.G. Indoor air quality in buildings: A comprehensive review on the factors influencing air pollution in residential and commercial structure. *Int. J. Environ. Res. Public Health.* **2021**, *18*, 3276. [CrossRef] [PubMed]
21. Lucialli, P.; Marinello, S.; Pollini, E.; Scaringi, M.; Zauli Sajani, S.; Marchesi, S.; Cori, L. Indoor and outdoor concentrations of benzene, toluene, ethylbenzene and xylene in some Italian schools—Evaluation of areas with different air pollution. *Atmos. Pollut. Res.* **2020**, *11*, 1998–2010. [CrossRef]
22. Yu, C.W.F.; Crump, D.R. Testing for formaldehyde emission from wood-based products—A review. *Indoor Built Environ.* **1999**, *8*, 280–286. [CrossRef]
23. Hodgson, A.T.; Beal, D.; McIlvaine, J.E.R. Sources of formaldehyde, other aldehydes and terpenes in a new manufactured house. *Indoor Air* **2002**, *12*, 235–242. [CrossRef]
24. Li, S.; Banyasz, J.L.; Parrish, M.E.; Lyons-Hart, J.; Shafer, K.H. Formaldehyde in the gas phase of mainstream cigarette smoke. *J. Anal. Appl. Pyrol.* **2002**, *65*, 137–145. [CrossRef]
25. Salthammer, T.; Mentese, S.; Marutzky, R. Formaldehyde in the indoor environment. *Chem. Rev.* **2010**, *110*, 2536–2572. [CrossRef] [PubMed]
26. Kelly, T.J.; Smith, D.L.; Satola, J. Emission rates of formaldehyde from materials and consumer products found in California homes. *Environ. Sci. Technol.* **1999**, *33*, 81–88. [CrossRef]
27. Chen, X.; Li, F.; Liu, C.; Yang, J.; Zhang, J.; Peng, C. Monitoring, Human Health Risk Assessment and Optimized Management for Typical Pollutants in Indoor Air from Random Families of University Staff, Wuhan City, China. *Sustainability* **2017**, *9*, 1115. [CrossRef]
28. Widder, S.H.; Haselbach, L. Relationship among Concentrations of Indoor Air Contaminants, Their Sources, and Different Mitigation Strategies on Indoor Air Quality. *Sustainability* **2017**, *9*, 1149. [CrossRef]
29. Soltanpour, Z.; Mohammadian, Y.; Fakhri, Y. The exposure to formaldehyde in industries and health care centers: A systematic review and probabilistic health risk assessment. *Environ. Res.* **2022**, *204 Part B*, 112094. [CrossRef]
30. Protano, C.; Antonucci, A.; De Giorgi, A.; Zanni, S.; Mazzeo, E.; Cammalleri, V.; Fabiani, L.; Mastrantonio, R.; Muselli, M.; Mastrangeli, G.; et al. Exposure and Early Effect Biomarkers for Risk Assessment of Occupational Exposure to Formaldehyde: A Systematic Review. *Sustainability* **2024**, *16*, 3631. [CrossRef]
31. Parrish, D.D.; Ryerson, T.B.; Mellqvist, J.; Johansson, J.; Fried, A.; Richter, D.; Walega, J.G.; Washenfelder, R.A.; de Gouw, J.A.; Peischl, J.; et al. Primary and secondary sources of formaldehyde in urban atmospheres: Houston Texas region. *Atmos. Chem. Phys.* **2012**, *12*, 3273–3288. [CrossRef]

32. Nogueira, T.; Dominutti, P.A.; De Carvalho, L.R.F.; Fornaro, A.; Andrade, M.D.F. Formaldehyde and acetaldehyde measurements in urban atmosphere impacted by the use of ethanol biofuel: Metropolitan Area of Sao Paulo (MASP), 2012–2013. *Fuel* **2014**, *134*, 505–513. [CrossRef]
33. Li, M.; Shao, M.; Li, L.-Y.; Lu, S.-H.; Chen, W.-T.; Wang, C. Quantifying the ambient formaldehyde sources utilizing tracers. *Chin. Chem. Lett.* **2014**, *25*, 1489–1491. [CrossRef]
34. Jung, S.; Kim, S.; Chung, T.; Hong, H.; Lee, S.; Lim, J. Emission Characteristics of Hazardous Air Pollutants from Medium-Duty Diesel Trucks Based on Driving Cycles. *Sustainability* **2021**, *13*, 7834. [CrossRef]
35. Giarracca, L.; Tran, L.-S.; Gosselin, S.; Hanoune, B.; Gasnot, L. Quantitative measurement of formaldehyde formed in combustion processes using gas chromatography analytical approach. *Combust. Sci. Technol.* **2023**, *195*, 2716–2731. [CrossRef]
36. Du, W.; Xie, H.; Li, J.; Guan, X.; Li, M.; Wang, H.; Wang, X.; Zhang, X.; Zhang, Q. The Emission Characteristics of VOCs and Environmental Health Risk Assessment in the Plywood Manufacturing Industry: A Case Study in Shandong Province. *Sustainability* **2024**, *16*, 7350. [CrossRef]
37. Goode, J.G.; Yokelson, R.J.; Ward, D.E.; Susott, R.A.; Babbitt, R.E.; Davies, M.A.; Hao, W.M. C_2H_2, HCN, NO, NH_3, HCOOH, CH_3COOH, HCHO, and CH_3OH in 1997 Alaskan biomass burning plumes by airborne Fourier transform infrared spectroscopy (AFTIR). *J. Geophys. Res. Atmos* **2000**, *105*, 22147–22166. [CrossRef]
38. Sinha, P.; Hobbs, P.V.; Yokelson, R.J.; Blake, D.R.; Gao, S.; Kirchstetter, T.W. Emissions from miombo woodland and dambo grassland savanna fires. *J. Geophys. Res. Atmos* **2004**, *109*, D11305. [CrossRef]
39. Na, K.; Cocker, D.R. Fine organic particle, formaldehyde, acetaldehyde concentrations under and after the influence of fire activity in the atmosphere of Riverside, California. *Environ. Res.* **2008**, *108*, 7–14. [CrossRef] [PubMed]
40. Young, E.; Paton-Walsh, C. Emission Ratios of the Tropospheric Ozone Precursors Nitrogen Dioxide and Formaldehyde from Australia's Black Saturday Fires. *Atmosphere* **2011**, *2*, 617–632. [CrossRef]
41. Sitnov, S.A.; Mokhov, I.I. Formaldehyde and nitrogen dioxide in the atmosphere during summer weather extremes and wildfires in European Russia in 2010 and western Siberia in 2012. *Int. J. Remote Sens.* **2017**, *38*, 4086–4106. [CrossRef]
42. Efimova, N.V.; Rukavishnikov, V.S. Assessment of Smoke Pollution Caused by Wildfires in the Baikal Region (Russia). *Atmosphere* **2021**, *12*, 1542. [CrossRef]
43. Simmons, J.B.; Paton-Walsh, C.; Mouat, A.P.; Kaiser, J.; Humphries, R.S.; Keywood, M.; Griffith, D.W.T.; Sutresna, A.; Naylor, T.; Ramirez-Gamboa, J. Bushfire smoke plume composition and toxicological assessment from the 2019–2020 Australian Black Summer. *Air Qual. Atmos. Health* **2022**, *15*, 2067–2089. [CrossRef]
44. Vichi, F.; Bassani, C.; Ianniello, A.; Esposito, G.; Montagnoli, M.; Imperiali, A. Formaldehyde Continuous Monitoring at a Rural Station North of Rome: Appraisal of Local Sources Contribution and Meteorological Drivers. *Atmosphere* **2023**, *14*, 1833. [CrossRef]
45. Zhao, T.; Mao, J.; Ayazpour, Z.; González Abad, G.; Nowlan, C.R.; Zheng, Y. Interannual variability of summertime formaldehyde (HCHO) vertical column density and its main drivers at northern high latitudes. *Atmos. Chem. Phys.* **2024**, *24*, 6105–6121. [CrossRef]
46. Adewuyi, Y.G.; Cho, S.-Y.; Tsay, R.-P.; Carmichael, G.R. Importance of formaldehyde in cloud chemistry. *Atmos. Environ.* **1984**, *18*, 2413–2420. [CrossRef]
47. Báez, A.P.; Padilla, H.G.; Belmont, R.D. Scavenging of atmospheric formaldehyde by wet precipitation. *Environ. Pollut.* **1993**, *79*, 271–275. [CrossRef] [PubMed]
48. Munger, J.W.; Jacob, D.J.; Danube, B.C.; Horowitz, L.W.; Keene, W.C.; Heikes, B.G. Formaldehyde, glyoxal, and methylglyoxal in air and cloudwater at a rural mountain site in central Virginia. *J. Geophys. Res. Atmos.* **1995**, *100*, 9325–9333. [CrossRef]
49. Borbon, A.; Ruiz, M.; Bechara, J.; Aumont, B.; Chong, M.; Huntrieser, H.; Mari, C.; Reeves, C.E.; Scialom, G.; Hamburger, T.; et al. Transport and chemistry of formaldehyde by mesoscale convective systems in West Africa during AMMA 2006. *J. Geophys. Res. Atmos.* **2012**, *117*, D12301. [CrossRef]
50. Fried, A.; Barth, M.C.; Bela, M.; Weibring, P.; Richter, D.; Walega, J.; Li, Y.; Pickering, K.; Apel, E.; Hornbrook, R.; et al. Convective transport of formaldehyde to the upper troposphere and lower stratosphere and associated scavenging in thunderstorms over the central United States during the 2012DC3 study. *J. Geophys. Res. Atmos.* **2016**, *121*, 7439–7460. [CrossRef]
51. Biswas, M.S.; Pandithurai, G.; Aslam, M.Y.; Patil, R.D.; Anilkumar, V.; Dudhambe, S.D.; Lerot, C.; De Smedt, I.; Van Roozendael, M. Effects of boundary layer evolution on nitrogen dioxide (NO_2) and formaldehyde (HCHO) concentrations at a high-altitude observatory in western India. *Aerosol Air Qual. Res.* **2021**, *21*, 200193. [CrossRef]
52. Ceccarelli, C.; Maret, S.; Tielens, A.G.G.M.; Castets, A.; Caux, E. Theoretical H_2CO emission from protostellar envelopes. *Astron. Astrophys.* **2003**, *410*, 587–595. [CrossRef]
53. Leroux, K.; Guillemin, J.-C.; Krim, L. Solid-state formation of CO and H_2CO via the CHOCHO + reaction. *Mon. Not. R. Astron. Soc.* **2020**, *491*, 289–301. [CrossRef]
54. Ramal-Olmedo, J.C.; Menor-Salván, C.A.; Fortenberry, R.C. Mechanisms for gas-phase molecular formation of neutral formaldehyde (H_2CO) in cold astrophysical regions. *Astron. Astrophys.* **2021**, *656*, A148. [CrossRef]
55. Ibrahim, M.; Guillemin, J.-C.; Chaquin, P.; Markovits, A.; Krim, L. Formation of CO, CH_4, H_2CO and CH_3CHO through the H_2CCO + H surface reaction under interstellar conditions. *Phys. Chem. Chem. Phys.* **2022**, *24*, 23245–23253. [CrossRef] [PubMed]
56. Berglund, B.; Johansson, I.; Lindvall, T. A longitudinal study of air contaminants in a newly built preschool. *Environ. Int.* **1982**, *8*, 111–115. [CrossRef]
57. Lee, S.C.; Chang, M. Indoor air quality investigations at five classrooms. *Indoor Air* **1999**, *9*, 134–138. [CrossRef]

58. Khoder, M.I.; Shakour, A.A.; Farag, S.A.; Abdel Hameed, A.A. Indoor and outdoor formaldehyde concentrations in homes in residential areas in Greater Cairo. *J. Environ. Monit.* **2000**, *2*, 123–126. [CrossRef]
59. Pegas, P.N.; Evtyugina, M.G.; Alves, C.A.; Nunes, T.; Cerqueira, M.; Franchi, M.; Pio, C.; Almeida, S.M.; Freitas, M.D.C. Outdoor/indoor air quality in primary schools in Lisbon: A preliminary study. *Quim. Nova* **2010**, *33*, 1145–1149. [CrossRef]
60. Goodman, N.B.; Wheeler, A.J.; Paevere, P.J.; Selleck, P.W.; Cheng, M.; Steinermann, A. Indoor volatile organic compounds at an Australian university. *Build. Environ.* **2018**, *135*, 344–351. [CrossRef]
61. Huang, K.; Song, J.; Feng, G.; Chang, Q.; Jiang, B.; Wang, J.; Sun, W.; Li, H.; Wang, J.; Fang, X. Indoor air quality analysis of residential buildings in northeast China based on field measurements and longtime monitoring. *Build. Environ.* **2018**, *144*, 171–183. [CrossRef]
62. Chang, T.; Wang, J.; Lu, J.; Shen, Z.; Huang, Y.; Sun, J.; Xu, H.; Wang, X.; Ren, D.; Cao, J. Evaluation of indoor air pollution during the decorating process and inhalation health risks in Xi'an, China: A case study. *Aerosol Air Qual. Res.* **2019**, *19*, 854–864. [CrossRef]
63. Liu, C.; Miao, X.; Li, J. Outdoor formaldehyde matters and substantially impacts indoor formaldehyde concentrations. *Build. Environ.* **2019**, *158*, 145–150. [CrossRef]
64. Abelmann, A.; McEwen, A.R.; Lotter, J.T.; Maskrey, J.R. Survey of 24-h personal formaldehyde exposures in geographically distributed urban office workers in the USA. *Environ. Sci. Pollut. Res. Int.* **2020**, *27*, 17250–27257. [CrossRef] [PubMed]
65. Kharel, M.; Chalise, S.; Chalise, B.; Sharma, K.R.; Gyawali, D.; Paudyal, H.; Neupane, B.B. Assessing volatile organic compound level in selected workplaces of Kathmandu Valley. *Heliyon* **2021**, *7*, e08262. [CrossRef]
66. Jung, C.; Alqassimi, N.; El Samanoudy, G. The comparative analysis of the indoor air pollutants in occupied apartments at residential area and industrial area in Dubai, United Arab Emirates. *Front. Built Environ.* **2022**, *8*, 998858. [CrossRef]
67. European Chemicals Agency. Substance Evaluation Conclusion as Required by REACH Article 48 and Evaluation Report for Formaldehyde. Available online: https://mail.isac.cnr.it/squirrelmail/src/webmail.php (accessed on 13 October 2024).
68. Salthammer, T. Formaldehyde in the ambient atmosphere: From an indoor pollutant to an outdoor pollutant? *Angew. Chem. Int. Ed.* **2013**, *52*, 3320–3327. [CrossRef] [PubMed]
69. Zhang, H.; Zheng, Z.; Yu, T.; Liu, C.; Qian, H.; Li, J. Seasonal and diurnal patterns of outdoor formaldehyde and impacts on indoor environments and health. *Environ. Res.* **2022**, *205*, 112550. [CrossRef]
70. Zhu, L.; Jacob, D.J.; Keutsch, F.N.; Mickley, L.J.; Scheffe, R.; Strum, M.; González Abad, G.; Chance, K.; Yang, K.; Rappenglück, B.; et al. Formaldehyde (HCHO) as a hazardous air pollutant: Mapping surface air concentrations from satellite and inferring cancer risks in the United States. *Environ. Sci. Technol.* **2017**, *51*, 5650–5657. [CrossRef]
71. Li, D.; Wang, S.; Xue, R.; Zhu, J.; Zhang, S.; Sun, Z.; Zhou, B. OMI-observed HCHO in Shanghai, China during 2010–2019 and ozone sensitivity inferred by improved HCHO/NO_2 ratio. *Atmos. Chem. Phys.* **2021**, *21*, 15447–15460. [CrossRef]
72. Butler, M.P.; Lauvaux, T.; Feng, S.; Liu, J.; Bowman, K.W.; Davis, K.J. Atmospheric Simulations of Total Column CO_2 Mole Fractions from Global to Mesoscale within the Carbon Monitoring System Flux Inversion Framework. *Atmosphere* **2020**, *11*, 787. [CrossRef]
73. Federico, S.; Pasqualoni, L.; De Leo, L.; Bellecci, C. A study of the breeze circulation during summer and fall 2008 in Calabria, Italy. *Atmos. Res.* **2010**, *97*, 1–13. [CrossRef]
74. Federico, S.; Pasqualoni, L.; Sempreviva, A.M.; De Leo, L.; Avolio, E.; Calidonna, C.R.; Bellecci, C. The seasonal characteristics of the breeze circulation at a coastal Mediterranean site in South Italy. *Adv. Sci. Res.* **2010**, *4*, 47–56. [CrossRef]
75. Gullì, D.; Avolio, E.; Calidonna, C.R.; Lo Feudo, T.; Torcasio, R.C.; Sempreviva, A.M. Two years of wind-lidar measurements at an Italian Mediterranean Coastal Site. In European Geosciences Union General Assembly 2017, EGU—Division Energy, Resources & Environment, ERE. *Energy Procedia* **2017**, *125*, 214–220. [CrossRef]
76. Avolio, E.; Federico, S.; Miglietta, M.M.; Lo Feudo, T.; Calidonna, C.R.; Sempreviva, A.M. Sensitivity analysis of WRF model PBL schemes in simulating boundary-layer variables in southern Italy: An experimental campaign. *Atmos. Res.* **2017**, *192*, 58–71. [CrossRef]
77. Lo Feudo, T.; Calidonna, C.R.; Avolio, E.; Sempreviva, A.M. Study of the Vertical Structure of the Coastal Boundary Layer Integrating Surface Measurements and Ground-Based Remote Sensing. *Sensors* **2020**, *20*, 6516. [CrossRef] [PubMed]
78. Cristofanelli, P.; Busetto, M.; Calzolari, F.; Ammoscato, I.; Gullì, D.; Dinoi, A.; Calidonna, C.R.; Contini, D.; Sferlazzo, D.; Di Iorio, T.; et al. Investigation of reactive gases and methane variability in the coastal boundary layer of the central Mediterranean basin. *Elem. Sci. Anth.* **2017**, *5*, 12. [CrossRef]
79. Calidonna, C.R.; Avolio, E.; Gullì, D.; Ammoscato, I.; De Pino, M.; Donateo, A.; Lo Feudo, T. Five Years of Dust Episodes at the Southern Italy GAW Regional Coastal Mediterranean Observatory: Multisensors and Modeling Analysis. *Atmosphere* **2020**, *11*, 456. [CrossRef]
80. Malacaria, L.; Parise, D.; Lo Feudo, T.; Avolio, E.; Ammoscato, I.; Gullì, D.; Sinopoli, S.; Cristofanelli, P.; De Pino, M.; D'Amico, F.; et al. Multiparameter detection of summer open fire emissions: The case study of GAW regional observatory of Lamezia Terme (Southern Italy). *Fire* **2024**, *7*, 198. [CrossRef]
81. D'Amico, F.; Ammoscato, I.; Gullì, D.; Avolio, E.; Lo Feudo, T.; De Pino, M.; Cristofanelli, P.; Malacaria, L.; Parise, D.; Sinopoli, S.; et al. Integrated analysis of methane cycles and trends at the WMO/GAW station of Lamezia Terme (Calabria, Southern Italy). *Atmosphere* **2024**, *15*, 946. [CrossRef]

82. D'Amico, F.; Gullì, D.; Lo Feudo, T.; Ammoscato, I.; Avolio, E.; De Pino, M.; Cristofanelli, P.; Busetto, M.; Malacaria, L.; Parise, D.; et al. Cyclic and multi-year characterization of surface ozone at the WMO/GAW coastal station of Lamezia Terme (Calabria, Southern Italy): Implications for local environment, cultural heritage, and human health. *Environments* **2024**, *11*, 227. [CrossRef]
83. Donateo, A.; Lo Feudo, T.; Marinoni, A.; Dinoi, A.; Avolio, E.; Merico, E.; Calidonna, C.R.; Contini, D.; Bonasoni, P. Characterization of In Situ Aerosol Optical Properties at Three Observatories in the Central Mediterranean. *Atmosphere* **2018**, *9*, 369. [CrossRef]
84. Donateo, A.; Lo Feudo, T.; Marinoni, A.; Calidonna, C.R.; Contini, D.; Bonasoni, P. Long-term observations of aerosol optical properties at three GAW regional sites in the Central Mediterranean. *Atmos. Res.* **2020**, *241*, 104976. [CrossRef]
85. D'Amico, F.; Ammoscato, I.; Gullì, D.; Avolio, E.; Lo Feudo, T.; De Pino, M.; Cristofanelli, P.; Malacaria, L.; Parise, D.; Sinopoli, S.; et al. Anthropic-induced variability of greenhouse gases and aerosols at the WMO/GAW coastal site of Lamezia Terme (Calabria, Southern Italy): Towards a new method to assess the weekly distribution of gathered data. *Sustainability* **2024**, *16*, 8175. [CrossRef]
86. D'Amico, F.; Ammoscato, I.; Gullì, D.; Avolio, E.; Lo Feudo, T.; De Pino, M.; Cristofanelli, P.; Malacaria, L.; Parise, D.; Sinopoli, S.; et al. Trends in CO, CO_2, CH_4, BC, and NO_x during the first 2020 COVID-19 lockdown: Source insights from the WMO/GAW station of Lamezia Terme (Calabria, Southern Italy). *Sustainability* **2024**, *16*, 8229. [CrossRef]
87. D'Amico, F.; Calidonna, C.R.; Ammoscato, I.; Gullì, D.; Malacaria, L.; Sinopoli, S.; De Benedetto, G.; Lo Feudo, T. Peplospheric influences on local greenhouse gas and aerosol variability at the Lamezia Terme WMO/GAW regional station in Calabria, Southern Italy: A multiparameter investigation. Under review at MDPI Sustainability.
88. European Space Agency. Overview of Sentinel-5P Mission. Available online: https://sentinel.esa.int/web/sentinel/missions/sentinel-5p (accessed on 16 October 2024).
89. De Smedt, I.; Theys, N.; Yu, H.; Danckaert, T.; Lerot, C.; Compernolle, S.; Van Roozendael, M.; Richter, A.; Hilboll, A.; Peters, E.; et al. Algorithm theoretical baseline for formaldehyde retrievals from S5P TROPOMI and from the QA4ECV project. *Atmos. Meas. Tech.* **2018**, *11*, 2395–2426. [CrossRef]
90. De Smedt, I.; Theys, N.; Yu, H.; Vlietinck, J.; he Lerot, C.; Roozendael, M.V. *S5P/TROPOMI HCHO ATBD*; Technical Report 2.3.0; BIRA-IASB: Uccle, Belgium, 2021.
91. Copernicus. Sentinel-2 L2 Database. Available online: https://browser.dataspace.copernicus.eu (accessed on 5 October 2024).
92. *ISO 7726*; Ergonomics of the thermal environment—Instruments for measuring physical quantities. International Organization for Standardization: Geneva, Switzerland, 1998.
93. Apituley, A.; Pedergnana, M.; Sneep, M.; Veefkind, J.P.; Loyola, D.H.O. *Sentinel-5 Precursor/TROPOMI Level 2 Product User Manual Methane*; Royal Netherlands Meteorological Institute: De Bilt, The Netherlands, 2022.
94. De Smedt, I.; Eichmann, K.U.; Lambert, J.C.; Loyola, D.; Veefkind, J.P. *S5P Mission Performance Centre Formaldehyde [L2 HCHO] Readme*; Technical Report; BIRA-IASB: Uccle, Belgium, 2019.
95. Vigouroux, C.; Langerock, B.; Augusto Bauer Aquino, C.; Blumenstock, T.; Cheng, Z.; De Mazière, M.; De Smedt, I.; Grutter, M.; Hannigan, J.W.; Jones, N.; et al. TROPOMI-Sentinel-5 Precursor formaldehyde validation using an extensive network of ground-based Fourier-transform infrared stations. *Atmos. Meas. Tech.* **2020**, *13*, 3751–3767. [CrossRef]
96. NIOSH. *National Occupational Research Agenda (NORA)/National Total Worker Health Agenda (2016–2026): A National Agenda to Advance Total Worker Health Research, Practice, Policy, and Capacity, April 2016*; U.S. Department of Health and Human Services, Centers for Disease Control and Prevention, National Institute for Occupational Safety and Health, DHHS (NIOSH) Publication 2016–114: Cincinnati, OH, USA, 2016. Available online: https://www.cdc.gov/niosh/docs/2016-114/pdfs/2016-114.pdf?id=10.26616/NIOSHPUB2016114 (accessed on 10 October 2024).
97. Spearman, C. The Proof and Measurement of Association between Two Things. *Am. J. Psychol.* **1904**, *15*, 72–101. [CrossRef]
98. Schober, P.; Boer, C.; Schwarte, L.A. Correlation Coefficients: Appropriate Use and Interpretation. *Anesth. Analg.* **2018**, *126*, 1763–1768. [CrossRef] [PubMed]
99. Myers, J.L.; Well, A.D.; Lorch, R.F., Jr. *Research Design and Statistical Analysis*, 3rd ed.; Routledge: New York, NY, USA, 2010; p. 832. [CrossRef]
100. de Blas, M.; Ibáñez, P.; García, J.A.; Gómez, M.C.; Navazo, M.; Alonso, L.; Durana, N.; Iza, J.; Gangoiti, G.; de Cámara, E.S. Summertime high resolution variability of atmospheric formaldehyde and non-methane volatile organic compounds in a rural background area. *Sci. Total Environ.* **2019**, *647*, 862–877. [CrossRef] [PubMed]
101. Freitas, A.D.; Fornaro, A. Atmospheric Formaldehyde Monitored by TROPOMI Satellite Instrument throughout 2020 over São Paulo State, Brazil. *Remote Sens.* **2022**, *14*, 3032. [CrossRef]
102. Maurya, N.K.; Pandey, P.C.; Sarkar, S.; Kumar, R.; Srivastava, P.K. Spatio-Temporal Monitoring of Atmospheric Pollutants Using Earth Observation Sentinel 5P TROPOMI Data: Impact of Stubble Burning a Case Study. *ISPRS Int. J. Geo-Inf.* **2022**, *11*, 301. [CrossRef]
103. Yombo Phaka, R.; Merlaud, A.; Pinardi, G.; Friedrich, M.M.; Van Roozendael, M.; Müller, J.-F.; Stavrakou, T.; De Smedt, I.; Hendrick, F.; Dimitropoulou, E.; et al. Ground-based Multi-AXis Differential Optical Absorption Spectroscopy (MAX-DOAS) observations of NO_2 and H_2CO at Kinshasa and comparisons with TROPOMI observations. *Atmos. Meas. Tech.* **2023**, *16*, 5029–5050. [CrossRef]

104. Wang, P.; Holloway, T.; Bindl, M.; Harkey, M.; De Smedt, I. Ambient Formaldehyde over the United States from Ground-Based (AQS) and Satellite (OMI) Observations. *Remote Sens.* **2022**, *14*, 2191. [CrossRef]
105. Qiu, S.; He, Z.; Liu, G.; Ding, Z.; Bu, Z.; Cao, J.; Ji, W.; Liu, W.; Su, C.; Wang, X.; et al. Ambient formaldehyde concentrations in summer in 30 Chinese cities and impacts on air cleaning of built environment. *Energy Built Environ.* **2024**, *5*, 493–499. [CrossRef]